

Rate Coefficients for the Thermal Decomposition of BrONO₂ and the Heat of Formation of BrONO₂

John J. Orlando* and Geoffrey S. Tyndall

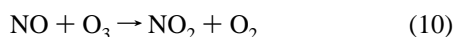
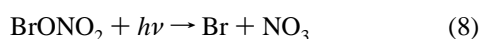
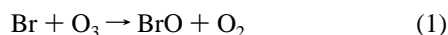
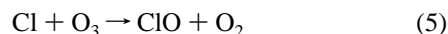
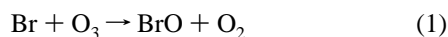
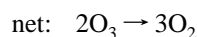
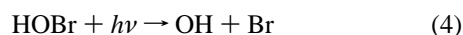
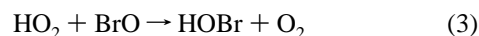
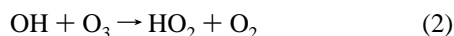
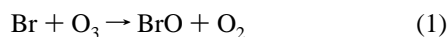
Atmospheric Chemistry Division, National Center for Atmospheric Research, Boulder, Colorado 80303

Received: July 8, 1996; In Final Form: October 4, 1996[⊗]

Rate coefficients (k_{-7}) for the thermal decomposition of bromine nitrate, BrONO₂ + M → BrO + NO₂ + M, have been obtained at temperatures between 320 and 340 K and pressures between 100 and 1000 Torr. These data are combined with recommended values for the reverse reaction to obtain an equilibrium constant for the reaction pair, $K_{p,7} = 5.44 \times 10^{-9} \exp(14192/T) \text{ atm}^{-1}$, and a heat of reaction for the thermal dissociation of $28.2 \pm 1.5 \text{ kcal/mol}$ at 298 K. This reaction enthalpy is used in conjunction with literature data to arrive at a consistent set of $\Delta H_f^\circ(298 \text{ K})$ data for BrONO₂ ($10.1 \pm 2.0 \text{ kcal/mol}$), BrO ($30.4 \pm 2.0 \text{ kcal/mol}$), HOBr ($-14.1 \pm 2.0 \text{ kcal/mol}$), and Br₂O ($27.3 \pm 2.0 \text{ kcal/mol}$). Additional measurements were made to determine the rate coefficient for Br atom reaction with BrONO₂ (k_{11}) relative to the rate coefficient for its reaction with CH₃CHO (k_{12}) at 298 K: $k_{11}/k_{12} = 12.5 \pm 0.6$. This relative rate measurement yields a rate coefficient of $(4.9 \pm 1.5) \times 10^{-11} \text{ cm}^3 \text{ molecule}^{-1} \text{ s}^{-1}$ for k_{11} , using the currently recommended value for k_{12} . Approximate rate constants for reaction of NO (reaction 17) and BrNO (reaction 19) with BrONO₂ were also obtained: $k_{17} = 3 \times 10^{-19} \text{ cm}^3 \text{ molecule}^{-1} \text{ s}^{-1}$, $k_{19} > 1 \times 10^{-16} \text{ cm}^3 \text{ molecule}^{-1} \text{ s}^{-1}$.

Introduction

The role of bromine in the destruction of ozone in the earth's stratosphere is now well characterized.^{1–5} Free bromine atoms are released from the destruction of source compounds such as CH₃Br and the halons and participate in catalytic ozone depleting cycles such as the following:



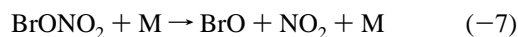
Bromine nitrate is thought to be an important component of

the inorganic bromine budget in the lower stratosphere. Rate coefficients for its formation via reaction 7 have been obtained over a range of temperatures and pressures,^{6–8} and the currently recommended values⁹ are obtained from the analysis of Thorn *et al.*⁸ Stratospheric loss of BrONO₂ is expected to occur largely via photolysis^{10,11} during the day, although the products of its photochemistry are not known. Heterogeneous loss of BrONO₂ on stratospheric aerosol is also rapid and may contribute to its loss during conditions of low sun.¹² While these data allow reasonably accurate determinations of its contribution to stratospheric chemistry, our understanding of the basic thermochemistry and reactivity of BrONO₂ is lacking.

To the best of our knowledge, the BrO–NO₂ bond strength has not yet been experimentally determined. Early estimates¹³ were based on the assumption that the BrO–NO₂ and ClO–NO₂ bond strengths were equal. Current recommendations⁹ give a $\Delta H_f^\circ(298 \text{ K})$ for thermal decomposition of ClONO₂ of 26.8 kcal/mol, based largely on the work of Anderson and Fahey.¹⁴ However, the low-pressure limiting rate coefficient, k_0 , for BrONO₂ formation is significantly larger than for the corresponding ClONO₂ formation reaction,^{8,9} possibly indicating a stronger bond in BrONO₂ than in ClONO₂. Also, measured values of k_0 are only slightly less than theoretical estimates^{7,8,13} of the strong-collision k_0 for BrONO₂ formation (and to a lesser extent for ClONO₂ formation), implying an unrealistically high collision efficiency. This inconsistency could be rationalized either by again assuming a stronger BrO–NO₂ bond than is the case for ClO–NO₂ or by invoking the formation of other isomers in the BrO + NO₂ recombination reaction. More recently, *ab initio* calculations¹⁵ have been performed which yield a BrO–NO₂ bond strength (35 kcal/mol) that is considerably larger than the accepted value for ClO–NO₂. While such a strong bond would explain the discrepancy between measured and calculated k_0 values, the *ab initio* calculations significantly overestimate the ClO–NO₂ bond strength (by about 6 kcal/mol), and though the trend obtained in the calculations of Rayez *et al.*¹⁵ is indicative of a stronger BrO–NO₂ bond, it is unlikely to be as strong as the *ab initio* value.

[⊗] Abstract published in *Advance ACS Abstracts*, November 15, 1996.

In this paper, we report rate coefficients for thermal decomposition of BrONO₂,

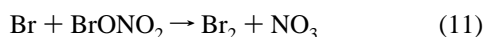


at $T = 320\text{--}340$ K and $P = 100\text{--}1000$ Torr. These data are combined with currently recommended rate constants for reaction 7 to determine the equilibrium constant, $K_7 = k_7/k_{-7}$, as a function of temperature and hence determine the BrO–NO₂ bond strength. The data are used to derive self-consistent ΔH_f° data for BrO, BrONO₂, HOBr, and Br₂O. During the course of these experiments, upper limits for the rate coefficients for unimolecular decay to Br + NO₃ and for isomer formation in the BrO + NO₂ + M reaction were obtained. Also, a rate coefficient for Br atom reaction with BrONO₂ (measured relative to Br + CH₃CHO) is reported, along with approximate rate coefficients for reaction of NO and BrNO with BrONO₂.

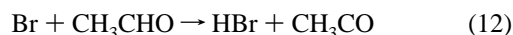
Experimental Section

1. Fourier Transform Spectrometer System. All experiments were conducted in a 2 m long, 47 L stainless steel chamber,^{16,17} interfaced to a BOMEM DA3.01 Fourier transform infrared spectrometer. The chamber is equipped with Hanst-type multipass optics which provided an IR analysis beam path length of 32.6 m. Water from a NESLAB Model EX-250HT bath was circulated around the cell to control the temperature. The temperature, as monitored by eight thermocouples along the length of the cell, was constant to ± 0.4 K. Fourier transform spectra, obtained from the coaddition of 5–50 scans, were typically recorded over the range 800–3900 cm⁻¹ at a spectral resolution of 1 cm⁻¹. Components of the gas mixtures—BrONO₂, CH₃CHO (Aldrich, 99%), NO (Linde), NO₂ (synthesized from addition of excess O₂ to NO), and Br₂ (Aldrich, 99.5%+)—were added to the cell via expansion from smaller calibrated volumes and flushed into the cell with O₂ (U.S. Welding, UHP Grade) or N₂ (boil-off from liquid N₂ Dewar). Calibration of IR spectra was achieved as follows: NO, NO₂, and CH₃CHO from comparison with standard spectra; N₂O₅ using the absorption cross sections of Cantrell *et al.*,¹⁸ CH₃C(O)O₂NO₂ (PAN) using the absorption cross sections of Tsalkani and Toupance,¹⁹ and BrONO₂ using absorption cross sections of Burkholder *et al.*¹¹ Burkholder *et al.* report absorption cross sections for the band near 800 cm⁻¹; absolute cross sections for the 1280 cm⁻¹ band were obtained in the current work from the simultaneous measurement of both bands. To accomplish this, BrONO₂ spectra were recorded in a 15 cm long Pyrex absorption cell which was housed in the sample compartment, which enabled spectra near 800 cm⁻¹ to be recorded with higher signal-to-noise ratios than is possible in the long path cell.

2. Experimental Procedures. *A. Rate Coefficient for Reaction of Br with BrONO₂.* Because the presence of Br atoms was anticipated in the thermal decomposition of BrONO₂ in the presence of NO, a reliable rate constant for Br with BrONO₂



was required to assess the contribution of this reaction in the study of the BrONO₂ thermolysis. The rate coefficient, k_{11} , was obtained relative to the known reaction rate coefficient for reaction of Br with CH₃CHO,



$k_{12} = 3.9 \times 10^{-12}$ cm³ molecule⁻¹ s⁻¹.²⁰ For these experiments, Br₂ ($\approx 10^{15}$ molecules/cm³) was photolyzed in the presence of BrONO₂ ($(3\text{--}5) \times 10^{13}$ molecules/cm³), CH₃CHO ($(5\text{--}8) \times$

10^{14} molecules/cm³), NO₂ ($\approx 10^{15}$ molecules/cm³), O₂ (50 Torr), and N₂ (650 Torr). Photolyses were performed with a Xe arc lamp, equipped with a Corning 3-74 filter ($\lambda > 410$ nm) to limit photolysis of NO₂.

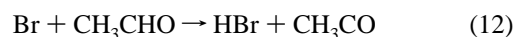
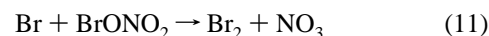
B. Thermal Decomposition of Bromine Nitrate. The thermal decomposition of BrONO₂ was studied by admitting BrONO₂, $(4\text{--}10) \times 10^{13}$ molecules/cm³, in the cell with NO, $(1\text{--}2) \times 10^{14}$ molecules/cm³, and N₂ (100–1000 Torr) and monitoring the temporal profile of BrONO₂, NO, and NO₂ via IR spectroscopy. Spectra were recorded at intervals of 25–45 s (depending on the rate of BrONO₂ decay) and consisted of 5–10 coadded scans. The heterogeneous loss of BrONO₂ was measured before and/or after each measurement of the thermal dissociation under the same conditions of temperature and pressure. These experiments were conducted by placing BrONO₂, $\approx (4\text{--}10) \times 10^{13}$ molecules cm⁻³, and NO₂, $\approx 2 \times 10^{15}$ molecules cm⁻³, in the cell with N₂.

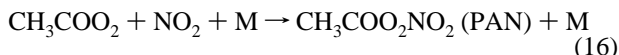
3. Materials. BrONO₂ was synthesized via the reaction of BrCl with ClONO₂, according to the method of Spencer and Rowland.¹⁰ ClONO₂ was prepared^{21,22} by combining Cl₂O (obtained from the reaction of Cl₂ with HgO powder) with excess N₂O₅ (prepared from reaction of O₃ with NO)¹⁸ at dry ice temperature and allowing the mixture to warm overnight to 273 K. The ClONO₂ was removed from the less volatile N₂O₅ by vacuum distillation at 195 K. BrCl was prepared by mixing Br₂ with excess Cl₂.¹¹ The BrCl was then condensed onto the ClONO₂ at dry ice temperature and allowed to stand for 1–2 days. This resulted in the conversion of a small fraction (<2%) of the ClONO₂ to BrONO₂. ClONO₂, BrCl, and Cl₂ were removed from the BrONO₂ by vacuum distillation. For this procedure, the ClONO₂/BrONO₂/BrCl/Cl₂ mixture was held at dry ice temperature and was pumped on through a liquid nitrogen trap. The more volatile Cl₂, ClONO₂, and BrCl were removed from the BrONO₂ and recondensed in the liquid nitrogen trap. This recondensed mixture was then allowed to stand for another 1–2 days at dry ice temperature, and the distillation process was repeated to obtain another BrONO₂ sample. The only impurity detected in the BrONO₂ via infrared spectroscopy was HNO₃, which was present at levels of 2–15%. No systematic variations in measured BrONO₂ decay rates with HNO₃ levels were noted; its presence as an impurity is not expected to interfere with any of the measurements reported here.

4. Chemical Modeling. Modeling of the experimental system was conducted using the ACUCHEM software.²³ Rate coefficients were obtained from recent evaluations^{9,20} when available; sources of other rate coefficients used in the model are noted in the text.

Results and Discussion

Rate Coefficient for Reaction of Br with BrONO₂. As described above, the rate coefficient for reaction 11 was determined relative to that for reaction 12 via photolysis of Br₂ in the presence of mixtures of CH₃CHO, BrONO₂, NO₂, O₂, and N₂. The relevant chemical reactions expected to occur in this system are as follows:





Reaction of Br with BrONO₂ then results in essentially stoichiometric production of N₂O₅ while reaction of Br with CH₃CHO leads to 1:1 formation of PAN. Successive irradiations were conducted for periods of 1–2 s, with IR spectra recorded after each irradiation. The rate coefficient for reaction 11 relative to reaction 12 was then obtained as follows:

$$-\frac{d[\text{BrONO}_2]}{dt} = k_{11}[\text{Br}][\text{BrONO}_2]$$

$$-\frac{d[\text{CH}_3\text{CHO}]}{dt} = k_{12}[\text{Br}][\text{CH}_3\text{CHO}]$$

$$\frac{d \ln[\text{BrONO}_2]}{d \ln[\text{CH}_3\text{CHO}]} = \frac{k_{11}}{k_{12}}$$

Because it was found that $k_{11} > k_{12}$, only small changes in CH₃CHO were observed. Hence, a more accurate means of determining the loss of CH₃CHO was through quantification of [PAN]: $[\text{CH}_3\text{CHO}]_t = [\text{CH}_3\text{CHO}]_0 - [\text{PAN}]_t$. At larger conversions, when CH₃CHO decay was quantifiable, this value was used directly for analysis. Small corrections to the BrONO₂ loss were made to account for its loss via heterogeneous processes, which was measured before each experiment.

Relative BrONO₂ and CH₃CHO loss rates are plotted against each other in Figure 1. These results are a compilation of five separate fills of the cell, with 2–5 irradiations performed per fill. A nonweighted linear least-squares fit of the data, as shown in Figure 1, yields the ratio $k_{11}/k_{12} = 12.5 \pm 0.6$. The negative intercept obtained in the fit is likely the result of imprecisions in the points obtained at low conversion, due to uncertainties in the correction for BrONO₂ wall loss and in the determination of the small CH₃CHO loss through quantification of PAN. Recent literature values for k_{12} at 298 K range from 3.5×10^{-12} to 4.45×10^{-12} molecules cm⁻³ s⁻¹,^{24–26} with a currently recommended value of 3.9×10^{-12} cm³ molecule⁻¹ s⁻¹.²⁰ Using this recommended rate coefficient yields a value of $(4.9 \pm 1.5) \times 10^{-11}$ cm³ molecules⁻¹ s⁻¹ for k_{11} , where the estimated uncertainty (1σ) includes precision (±5%), systematic uncertainties (±15%) in the relative rate determination (including uncertainties in the IR band strength of PAN and CH₃CHO), and the estimated uncertainty in the reference rate coefficient (±10%). Soller et al.²⁷ have recently reported $k_{11} = 2.08 \times 10^{-11} \exp(320/T)$, in agreement with our room temperature value.

Reaction of BrONO₂ with NO and BrNO. During the course of this work, other reactions of BrONO₂ were discovered. It was initially thought that the optimum conditions for conducting the thermal decomposition experiments would be in a large excess of NO over BrONO₂. Under these conditions, the NO₂ to NO concentration ratio would remain low, and re-formation of BrONO₂ via reaction 7 would not occur. Also, the large NO concentration would provide a sink for Br atoms and remove the uncertainty associated with the occurrence of reaction 11, for which no rate coefficient data were originally available. However, addition of large quantities of NO (of order 10 Torr) to BrONO₂ samples resulted in rapid consumption of the BrONO₂, with concomitant formation of NO₂ and BrNO. The observations were consistent with a relatively slow reaction of BrONO₂ with NO,

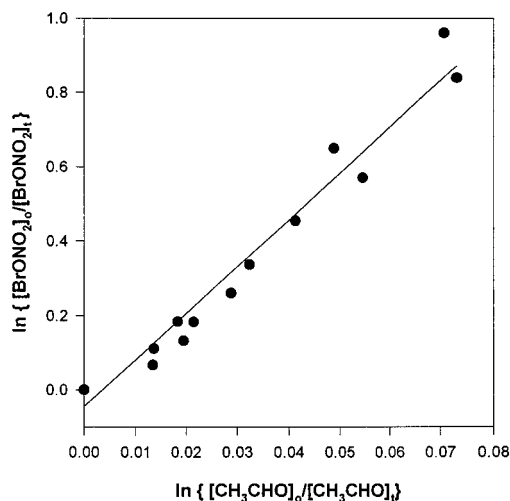


Figure 1. Relative loss of BrONO₂ and CH₃CHO observed in the photolysis of Br₂/CH₃CHO/BrONO₂/NO₂/O₂ mixtures. Solid line represents a linear least-squares fit to the data.

followed by reaction of NO₃ with NO,

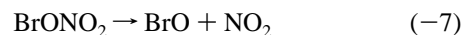


to produce NO₂. Experiments conducted in a more controlled fashion (with less NO) failed to reveal BrNO as a product and were suggestive of a reaction of BrNO with BrONO₂ leading to NO₂ formation,

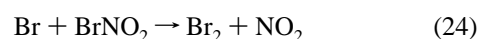
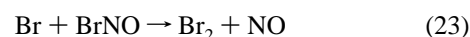


The results of all experiments can be explained if reaction 17 proceeds with a rate coefficient of about 3×10^{-19} cm³ molecule⁻¹ s⁻¹ and reaction 19 proceeds with a rate coefficient $\geq 10^{-16}$ cm³ molecule⁻¹ s⁻¹. Analogous reactions of ClONO₂ with NO, $k = 2.1 \times 10^{-12} \exp(-5966/T)$ cm³ molecule⁻¹ s⁻¹, and with ClNO, $k = 2 \times 10^{-20}$ cm³ molecule⁻¹ s⁻¹ at 343 K, have been reported by Knauth.²⁸

Thermal Decay Rates of BrONO₂. BrONO₂ loss in the presence of NO was found to obey first-order kinetics, with observed loss rates of 10^{-3} – 10^{-2} s⁻¹ for the range of conditions studied here (320 K < T < 340 K, 100–1000 Torr total pressure). Experiments were conducted in the presence of NO as described in the experimental section, in order to convert BrO to Br and hence stop the re-formation of BrONO₂ via reaction 7:

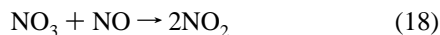


Concentrations of NO were kept below 2×10^{14} molecules cm⁻³ to minimize the occurrence of reaction 17. The Br atoms produced in reaction 20 would then be expected to react with BrONO₂ (reaction 11), with NO, NO₂, BrNO, and BrNO₂:



Under the conditions employed in these experiments, the predominant fate of the Br-atoms is reaction with BrONO₂

(reaction 11, $k_{11} = 4.9 \times 10^{-11} \text{ cm}^3 \text{ molecule}^{-1} \text{ s}^{-1}$, see above). The NO₃ produced in reaction (11) would rapidly react with NO,



Hence, thermal dissociation of a BrONO₂ molecule actually leads to the consumption of a second BrONO₂. To a first approximation, the overall stoichiometry (given by the sum of reactions -7, 20, 11, and 18) should then be as follows:



The infrared spectra confirmed that this stoichiometry was obeyed. On average, 1.9 ± 0.3 molecules of NO₂ were produced and 0.9 ± 0.2 molecules of NO consumed per BrONO₂ lost. No evidence for production of BrNO or BrNO₂ was found in any of the experiments conducted, supporting the hypothesis that Br atoms produced in this system were reacting with BrONO₂ and hence that about two BrONO₂ molecules are lost per thermal dissociation event.

BrONO₂ was also susceptible to loss at the cell walls, a process that needed to be accounted for in the analysis of the thermal dissociation data. As described in the Experimental Section, experiments were conducted in the presence of NO₂ to determine the rate of this process. Under these conditions, thermal dissociation to BrO and NO₂ in the presence of NO₂ is quickly followed by re-formation of BrONO₂ via reaction 7 and hence leads to no BrONO₂ loss. Hence, loss of BrONO₂ is most likely dominated by nonreversible loss at the walls of the cell. Decay of the BrONO₂ was found to be considerably slower ($\approx 10^{-4} \text{ s}^{-1}$) than for experiments conducted in the presence of NO.

Rate constants for reaction -7 for each experiment were obtained from a box model simulation of the reaction system, in order to accurately account for the contributions of reactions 7, 11, and 17 to the BrONO₂ temporal profile. For these simulations, the heterogeneous loss rate of BrONO₂ was fixed at the value measured in the presence of NO₂, and the rate coefficient for k_{-7} was adjusted in the model to obtain the best match to the observed BrONO₂ temporal profile. For typical conditions, the observed loss of BrONO₂ was 1.8–1.9 times the value of k_{-7} extracted from the model, again showing the importance of reaction 11 in determining the BrONO₂ temporal profile. Modeling tests showed that the extracted values of k_{-7} were not particularly sensitive to the value of k_{11} —decreasing this rate coefficient by an order of magnitude changed the value of k_{-7} by less than 15%.

The values of k_{-7} obtained from the simulations at each temperature and pressure studied are given in Table 1. The data recorded at 700 Torr pressure are plotted in Arrhenius form in Figure 2. Linear least-squares analysis yields the following best fit line (also shown in Figure 2): $\ln(k_{-7}) = 30.96 - 12360/T$. Of course, this relationship is only applicable at 700 Torr total pressure as the reaction is in the falloff region between first- and second-order kinetics at this pressure.

The pressure dependence of k_{-7} was investigated at 336 K at pressures between 100 and 1000 Torr (see Figure 3). The line shown is obtained by dividing the rate coefficient data for k_7 (obtained from the parameters of refs 8 and 9) by the equilibrium constant $K_{p,7}$ derived below ($K_{p,7} = 5.44 \times 10^{-9} \exp(14192/T) \text{ atm}^{-1}$). The agreement with the falloff is excellent, indicating that the pressure dependence observed in this work agrees well with that measured for the formation reaction 7.

TABLE 1: Kinetic Data Used and Results Obtained in the Third Law Analysis of BrONO₂ Dissociation Rates

temp (K)	press. (Torr)	k_{-7}^a (s ⁻¹)	k_7^b (cm ³ s ⁻¹)	K_p (atm ⁻¹)	$\ln(K_p)$	$-\Delta H_r^\circ$ (kcal/mol)
340.2	700	6.00E-03 ^c	1.73E-12	6.23E+09	22.552	-28.11
333.9	700	1.90E-03	1.85E-12	2.14E+10	23.788	-28.41
325.2	700	9.30E-04	2.03E-12	4.93E+10	24.622	-28.21
328.0	700	1.40E-03	1.97E-12	3.15E+10	24.174	-28.16
328.4	700	1.30E-03	1.96E-12	3.37E+10	24.242	-28.24
331.8	700	2.20E-03	1.89E-12	1.90E+10	23.669	-28.15
338.0	700	3.40E-03	1.77E-12	1.13E+10	23.150	-28.33
336.0	700	3.10E-03	1.81E-12	1.28E+10	23.270	-28.24
335.4	700	3.90E-03	1.82E-12	1.02E+10	23.048	-28.04
336.0	700	2.35E-03	1.81E-12	1.68E+10	23.547	-28.43
336.0	125	1.25E-03	7.00E-13	1.22E+10	23.229	-28.21
339.7	700	4.00E-03	1.74E-12	9.41E+09	22.965	-28.35
339.6	700	4.00E-03	1.74E-12	9.41E+09	22.965	-28.34
339.7	700	3.70E-03	1.74E-12	1.02E+10	23.043	-28.40
336.0	1000	3.20E-03	2.22E-12	1.52E+10	23.443	-28.36
335.9	100	8.80E-04	6.34E-13	1.58E+10	23.481	-28.37
336.0	300	1.40E-03	1.18E-12	1.84E+10	23.637	-28.49
320.0	700	4.70E-04	2.15E-12	1.05E+11	25.378	-28.24
323.0	700	5.70E-04	2.08E-12	8.30E+10	25.142	-28.35
324.2	700	7.00E-04	2.05E-12	6.64E+10	24.919	-28.31
322.1	700	6.10E-04	2.10E-12	7.85E+10	25.087	-28.23

^a Values measured in this work. ^b Determined from parameters given in ref 9, for the pressure and temperature at which k_{-7} was measured. ^c Read as 6.00×10^{-3} .

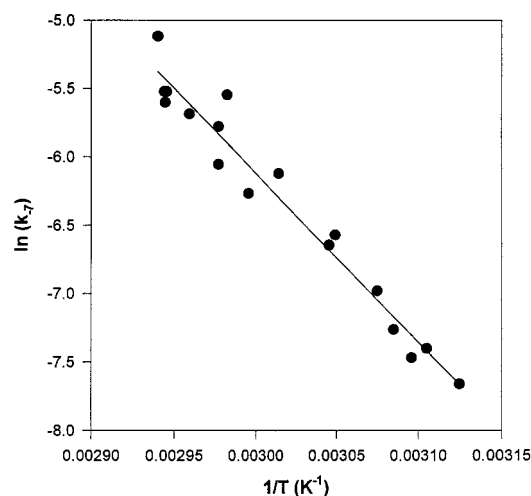


Figure 2. Plot of the dissociation rate of BrONO₂ as a function of inverse temperature, for all measurements made near 700 Torr. Solid line represents a linear least-squares fit to the data.

These BrONO₂ dissociation rate coefficients are considerably slower than those for the analogous dissociation of ClONO₂.^{14,29,30} As a check of our experimental system, and as a check of previously measured values of ClONO₂ thermal dissociation,^{14,29,30} this process was investigated briefly as a function of pressure at an arbitrarily selected temperature of 323 K in a method similar to that used to study reaction -7. Shown in Figure 4 are data for dissociation of ClONO₂ at pressures ranging from 100 to 800 Torr at 323 K. Also shown in Figure 4 are the predicted dissociation rate constants, obtained from the combination of the equilibrium constant recommended by Anderson and Fahey¹⁴ with the formation rate constants recommended by the NASA Panel.⁹ Since the measurements agreed within their uncertainty with the calculated values, no further experiments were performed. However, it is clear that the dissociation of ClONO₂ is considerably faster than that of BrONO₂ (about 10^{-2} s^{-1} at 323 K, 700 Torr for ClONO₂, compared to 3×10^{-3} at 336 K, 700 Torr for BrONO₂). As will be presented in detail later, this is largely due to a stronger XO–NO₂ bond in BrONO₂ than in ClONO₂.

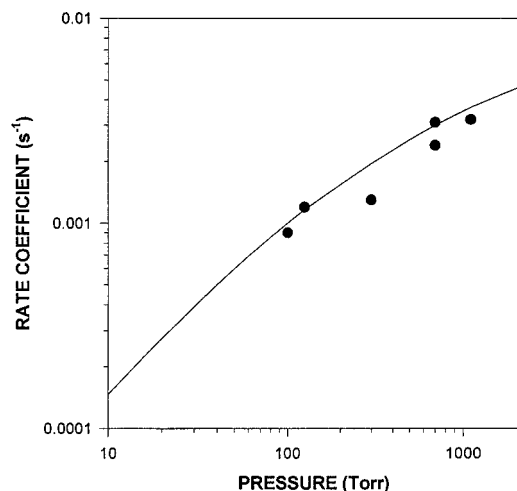


Figure 3. Dissociation rate of BrONO_2 as a function of pressure, for measurements made at 336 ± 0.2 K. (●) Measured dissociation rates. The solid line is obtained by dividing k_7 data from ref 8 by the equilibrium constant, K_7 , obtained in this work.

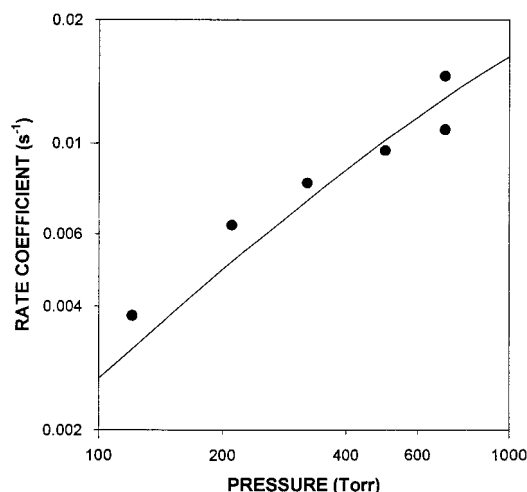


Figure 4. Dissociation rate of ClONO_2 as a function of pressure at 323 K. (●) Measured dissociation rates. The solid line is obtained by dividing the equilibrium constant for $\text{ClONO}_2 \rightleftharpoons \text{ClO} + \text{NO}_2$ from ref 14 by $\text{ClO} + \text{NO}_2 + \text{M}$ rate coefficient data from ref 9.

Decomposition of BrONO_2 to Br and NO_3 is possible,



although it is unlikely due to the fact that it is more endothermic than reaction -7. Experiments conducted in the presence of NO_2 (to determine the wall loss) can also be analyzed to obtain an upper limit for this process. Under conditions employed in these experiments, NO_3 produced via reaction 25 would be converted via reaction 14 to N_2O_5 ; the Br atom would react at least in part with BrONO_2 via reaction 11, generating another NO_3 and hence another N_2O_5 . No N_2O_5 was observed by IR spectroscopy in any of these experiments, indicating that decomposition to $\text{Br} + \text{NO}_3$ (reaction 25) occurs at a rate that is at least 25 times slower than decomposition via reaction -7.

These same experiments conducted in the presence of NO_2 can be used to consider the possibility of formation of products other than BrONO_2 in reaction 7. In these experiments, BrONO_2 decomposition and re-formation occurs a number of times before the heterogeneous reaction results in nonreversible BrONO_2 loss. For typical experiments conducted here, the thermal dissociation occurred at a rate that was about 4–5 times faster than the loss rate assigned to the heterogeneous reaction.

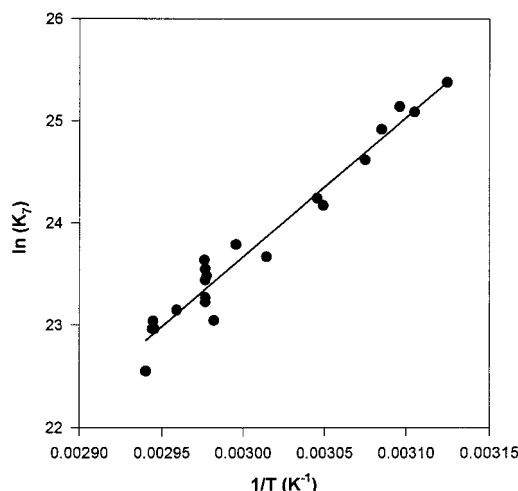


Figure 5. Equilibrium constant (K_7) plotted as a function of inverse temperature. The linear least-squares fit (second law analysis) gives ΔH_r° of 27.1 ± 2.6 kcal/mol. Third law analysis of the same data yields $\Delta H_r^\circ = 28.2 \pm 1.5$ kcal/mol.

Thus, even if all the loss assigned to heterogeneous processes is actually due to formation of some species other than BrONO_2 , the rate coefficient for this other reaction can at most be a factor of 4 less than that for reaction 7 under the conditions of temperature and pressure studied herein. This is almost certainly an upper limit, since no evidence for other products is obtained from the IR spectra. This type of experiment is the first to show that BrONO_2 is indeed the major product of BrO/NO_2 recombination (at least at the temperatures and pressures employed here).

Determination of the $\Delta H_r^\circ(298 \text{ K})$ and $\Delta S_r^\circ(298 \text{ K})$ for BrONO_2 Thermal Dissociation. In order to properly assess the thermodynamics involved in the reaction system, analysis was performed using both the “second law” and “third law” methods. Both of these analyses require the calculation of equilibrium constants $K_{p,7} = k_7/k_{-7}(RT)^{-1}$. These values (obtained using the measured k_{-7} and values for k_7 from the recommended parameters)^{9,20} are presented in Table 1. In the second law analysis, the well-known relationship

$$-\ln(K_{p,7}) = \left(\frac{\Delta H_r^\circ}{R}\right)\frac{1}{T} - \left(\frac{\Delta S_r^\circ}{R}\right)$$

is employed. Figure 5 shows a plot of $\ln K_{p,7}$ as a function of inverse temperature. The slope of this plot, as obtained by nonweighted linear least-squares analysis, gives a value of ΔH_r° for the decomposition reaction at a temperature of 335 K (the mean of the temperature range studied here) of 27.1 ± 2.6 kcal/mol (2σ precision error only). Correction of this value to 298 K is negligible (<0.1 kcal/mol), and hence the reaction enthalpy at 298 K is adequately represented by the value obtained from the fit. The intercept of this second-order plot yields an entropy change, ΔS_r° , for this reaction of $34.3 \text{ cal K}^{-1} \text{ mol}^{-1}$. Comparison of these values with those obtained by the third law method will be made below.

In the “third law” analysis, each individual determination of $K_{p,7}$ in Table 1 is used to determine $\Delta H_r^\circ(298 \text{ K})$ as follows:^{14,31}

$$\Delta H_r^\circ(298 \text{ K}) = -RT \ln[K_{p,7}(T)] - \sum [-TS^\circ(T) + [H^\circ(T) - H^\circ(298 \text{ K})]]$$

where the summation is over products minus reactants. Values of $S^\circ(T)$ and $[H^\circ(T) - H^\circ(298 \text{ K})]$ for NO_2 were obtained from

TABLE 2: Thermodynamic and Kinetic Data for the Halogen Nitrates (All Data at 298 K)

	ΔH_f° for XONO ₂ (kcal/mol)	XO–NO ₂ bond strength (kcal/mol)	X–O bond strength (kcal/mol)	X–ONO ₂ bond strength (kcal/mol)	k_0 (formation) (cm ⁶ molec ⁻² s ⁻¹)	β_c
X = F	3.1 ± 2.0 ^a	31 ± 5 ^b	52.6 ± 5 ^b	33.5 ± 2.0 ^b	2.6 × 10 ⁻³¹ c	0.4 ^d
X = Cl	5.5 ^c	26.8 ^c	64.1 ^c	41.0 ^c	1.8 × 10 ⁻³¹ c	0.6 ^d
X = Br	10.1 ± 1.5 ^e	28.2 ± 1.5 ^f	55.9 ± 1.5 ^e	34.2 ± 1.5 ^e	5.2 × 10 ⁻³¹ c	0.7 ^f
X = I	<9.5 ^g (7 ± 2) ^h	>25.4 ^g (28 ± 2) ^h	58 ± 2 ⁱ	>33.6 ^g (36.5 ± 2) ^h	5.9 × 10 ⁻³¹ c	

^a From *ab initio* calculation of ref 44. ^b Using ΔH_f° value of ref 44, with ΔH_f° values for O, F, FO, NO₂, and NO₃ from ref 9. ^c From ref 9. ^d From ref 15. ^e Using BrONO₂ + H₂O ⇌ HOBr + HNO₃ equilibrium constant measurement of ref 34, BrO–NO₂ bond strength from this work, an average ΔH_f° for HOBr from refs 38, 39, and 42, and ΔH_f° values for O, Br, NO₂, and NO₃ from ref 9 (see text for details). ^f This work. ^g Using upper limit to ΔH_f° for IONO₂ from kinetics study of ref 45, estimated ΔH_f° for IO of 27 kcal/mol, and ΔH_f° values for I, I₂, NO₂, and NO₃ from ref 9. ^h Based on estimated I–ONO₂ bond strength (see text), estimated ΔH_f° for IO of 27 kcal/mol, and ΔH_f° values for I, NO₂, and NO₃ from ref 9. ⁱ From an estimated value for ΔH_f° for IO of 27 kcal/mol, which is the middle of the range of values reported in refs 9, 20, and 46–50 and ΔH_f° values for I and O from ref 9.

interpolation of the JANAF tables,³¹ while values for BrO and BrONO₂ were calculated from known (or estimated) spectroscopic parameters, using methods outlined by Chase *et al.*³¹ Spectroscopic parameters for BrO were obtained from Orlando *et al.*,³² while those for BrONO₂ were obtained from Spencer and Rowland,¹⁰ Sander *et al.*,⁶ and Patrick and Golden.¹³ The average value for ΔH_f° (298 K) from the third law method is 28.2 ± 0.2 kcal/mol (2σ precision error only).

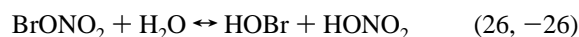
Thus, the ΔH_f° (298 K) values for BrONO₂ dissociation obtained by second law and third law analysis agree within the uncertainties of the two analyses. Because of the larger uncertainty associated with obtaining ΔH_f° from the second law analysis over such a narrow temperature range, the value obtained from the third law analysis is recommended.³¹ However, additional uncertainties (other than the precision error) exist in this third law value which will now be discussed. First, we estimate a possible ±20% systematic error in the measured values of k_{-7} associated with potentially unforeseen secondary chemistry not properly accounted for in the simulations. Second, values of k_7 used in the calculation of K_7 have a ±15% uncertainty associated with them. These two factors contribute a combined uncertainty of ±0.3 kcal/mol to the ΔH_f° value. Finally, the two lowest frequency BrONO₂ vibrations have not been observed and are obtained from estimates.⁶ Variation of these frequencies by a factor of 2 from the estimated values leads to an uncertainty of ±1.0 kcal/mol in the ΔH_f° value. Combining these uncertainties, we report a ΔH_f° (298 K) value of 28.2 ± 1.5 kcal/mol. From the third law analysis, the value of ΔS_r° for reaction -7 is found to be 37.8 cal K⁻¹ mol⁻¹. Since these ΔH_f° and ΔS_r° are essentially independent of temperature over the range studied, an equilibrium constant of $K_{P,7} = 5.44 \times 10^{-9} \exp(14192/T) \text{ atm}^{-1}$ can be obtained.

To the best of our knowledge, this is the first experimentally determined value for the BrO–NO₂ bond strength in BrONO₂. Patrick and Golden¹³ reported a value for this bond strength of 26.7 kcal/mol, but this was estimated by analogy to ClONO₂. More recently, Rayez and Destriau¹⁵ conducted both *ab initio* and semiempirical calculations to determine the XO–NO₂ bond strengths for X = F, Cl, Br, and I. They report an *ab initio* value of 34.2 kcal/mol for BrO–NO₂ at 0 K (which extrapolates to 35 kcal/mol at 298 K), significantly higher than our value. It is worth noting, however, that while their *ab initio* value agrees with experiment for FONO₂, the *ab initio* value for ClONO₂ is some 5 kcal/mol higher than experiment. Thus, it is apparent that the trend determined in the *ab initio* calculations is semiquantitatively correct but that the absolute values of the ClO–NO₂ and BrO–NO₂ bond strength are overestimated by the *ab initio* method. The semiempirical value for BrONO₂ decomposition obtained by Rayez and Destriau is considerably larger than either their *ab initio* value or our experimentally determined value.

Heat of Formation for BrONO₂. There is considerable uncertainty in the ΔH_f° values for BrO, HOBr, and BrONO₂, all of which are of importance in atmospheric chemistry. Experiments (such as the one conducted here) often determine the difference between the heats of formation of the various species, making absolute values difficult to obtain. Nonetheless, it appears that sufficient information is now available from which a consistent set of ΔH_f° values for BrO, HOBr, and BrONO₂ can be obtained.

The simplest approach to the determination of ΔH_f° (298 K) for BrONO₂ from the experiments conducted here is to combine the measured heat of reaction -7 with known values of ΔH_f° (298 K) for BrO and NO₂. While the value for NO₂ is well-known, 7.9 ± 0.2 kcal/mol,⁹ less confidence can be applied to the BrO value. The IUPAC panel,²⁰ based on spectroscopic work of Durie and Ramsay,³³ recommend ΔH_f° (298 K) = 30 kcal/mol for BrO. However, in their most recent evaluation, the NASA Panel⁹ recommend 26 ± 5 kcal/mol. Because there is no direct experimental evidence to contradict the Durie and Ramsay³³ estimate, we choose at this point to use the value of 30 kcal/mol obtained from their analysis. This leads to a value of 9.7 ± 2.0 kcal/mol for the ΔH_f° (298 K) of BrONO₂. Owing to the stronger BrO–NO₂ bond determined here compared to previous estimates, the ΔH_f° value is somewhat lower than previous recommendations.^{9,20}

An alternative approach is provided by the recent work of Hanson *et al.*,³⁴ who studied the equilibrium process



and report ΔH_f° (298 K) for the forward reaction 26 to be 1.3 ± 0.7 kcal/mol. The ΔH_f° value for HOBr has been the subject of numerous recent investigations;^{35–42} the most direct measurements^{38,39,42} yield an average value of -14.1 kcal/mol. Use of this value for HOBr and the ΔH_f° value for reaction 26 of 1.3 ± 0.7 kcal/mol yields a ΔH_f° (298 K) for BrONO₂ of 10.1 ± 0.8 kcal/mol, in agreement with the value determined above. This independent value of ΔH_f° (298 K) for BrONO₂, combined with the BrO–NO₂ bond strength determined here, can be used to determine a ΔH_f° (298 K) value for BrO of 30.4 ± 2 kcal/mol, thus confirming the value reported by Durie and Ramsay.³³ Although the two methods outlined above for determination of the heats of formation of the various bromine species are entirely self-consistent, the ΔH_f° of HOBr would seem to be better characterized than that of BrO, and the latter data are recommended. Finally, a study of the Br₂O/H₂O/HOBr equilibrium system³⁵ allows a value of 27.3 ± 2 kcal/mol to be obtained for ΔH_f° (298 K) of Br₂O, consistent with recently reported values of 25.6 ± 1.7⁴⁰ and 29.1 ± 1.0 kcal/mol.⁴³

Evaluation of Related Thermodynamic and Kinetic Data. Table 2 gives heats of formation for the halogen nitrates, as

well as X–O, X–ONO₂, and XO–NO₂ bond strengths and low-pressure rate coefficients (k_0) for formation of the halogen nitrates. It is seen that the ratio of the X–O bond strengths in XONO₂ and XO (for X = F, Cl, Br) is constant, 0.63 ± 0.02 . This is similar to the correlation reported by Zhang et al.⁵¹ for X–O and X–OH bond strengths. If it is assumed that this correlation extends to iodine, an estimate of the I–ONO₂ bond strength of 36.5 ± 2.0 kcal/mol can be made. This leads to a value of 7 ± 2 kcal/mol for $\Delta H_f^\circ(298\text{ K})$ of IONO₂, assuming $\Delta H_f^\circ(298\text{ K})$ for IO is 27 kcal/mol, the midrange of recently reported values.^{7,20,46–50} This is consistent with the best available estimate for ΔH_f° for IONO₂ of <9.5 kcal/mol, which is obtained from the observation⁴⁵ of a rapid reaction between I₂ and NO₃ (see Table 2).

Theoretical values for k_0 can be obtained from the statistical adiabatic channel model (SACM) method.^{7,13,15,52–54} In these calculations, a strong collision rate coefficient (k_0^{sc}) is obtained, which is related to the measured k_0 by a factor β_c (the collision efficiency, $\beta_c < 1$): $k_0(\text{measured}) = \beta_c k_0^{\text{sc}}$. Values of β_c for N₂ bath gas are typically in the range 0.1–0.3. Table 2 gives updated values for β_c for the halogen nitrates obtained using the most recent XO–NO₂ bond strengths; values for FONO₂ and ClONO₂ are taken from Rayez and Destriau¹⁵ since the bond strengths employed in those calculations are in agreement with current literature. For the calculation of β_c for BrONO₂, the value given by Rayez and Destriau was scaled to the present bond dissociation energy. The Rayez and Destriau¹⁵ determination of a stronger BrO–NO₂ bond led to a calculated β_c of ≈ 0.2 and seemed to resolve the discrepancy between measured and calculated k_0 values for reaction 7. However, our measurements of a weaker BrO–NO₂ bond than calculated by Rayez and Destriau (but stronger than the measured ClO–NO₂ bond) leads to a higher value for β_c , 0.7. Indeed, values of β_c fall in the range 0.4–0.7 for the entire series, somewhat higher than might be expected. Calculated values of β_c for the very similar reaction between HO₂ and NO₂



are also higher than expected, $\beta_c = 0.9$,¹³ as are calculated values for k_∞ for the entire series of XO + NO₂ reactions;¹⁵ no reason has been presented for the fact that rate coefficients for this set of related reactions are higher than predicted. It is clear from the present work that formation of isomers other than BrONO₂ cannot explain the faster than expected value for k_7 .

Conclusions

Rate coefficients for the thermal dissociation of BrONO₂ have been measured between 320 and 340 K, in the presence of 100–1000 Torr of N₂. The data were analyzed to show that BrO and NO₂ are the main products of the dissociation and that the major (if not sole) product of their recombination is BrONO₂. The dissociation rate coefficients were used to determine a value of 28.2 kcal/mol for the BrO–NO₂ bond strength at 298 K. This value is significantly lower than a recently published *ab initio* calculation, but higher than the experimentally determined value for the analogous ClO–NO₂ bond. Combining this measurement with recent literature data leads to a self-consistent set of ΔH_f° data for BrO, HOBr, BrONO₂, and Br₂O. Finally, rate coefficients for reaction of Br ($(4.9 \pm 1.5) \times 10^{-11}$ cm³ molecule⁻¹ s⁻¹), NO ($\approx 3 \times 10^{-19}$ cm³ molecule⁻¹ s⁻¹), and BrNO ($\geq 10^{-16}$ cm³ molecule⁻¹ s⁻¹) with BrONO₂ were obtained.

Acknowledgment. This work was supported by NASA Upper Atmospheric Research Program, under Contract W-18067.

Thanks are due to Lee Mauldin and Chris Cantrell for helpful comments on the manuscript. We are indebted to Jim Burkholder (NOAA Aeronomy Laboratory) for helpful hints in the preparation and handling of BrONO₂ and to Jim Burkholder, Dave Hanson, A. R. Ravishankara, and Ned Lovejoy (all of the NOAA Aeronomy Lab) for helpful discussions regarding BrONO₂, HOBr, and BrO thermochemistry and for communication of results prior to publication. NCAR is partially supported by the NSF.

References and Notes

- (1) Yung, Y. L.; Pinto, J. P.; Watson, R. T.; Sander, S. P. *J. Atmos. Sci.* **1980**, *37*, 339.
- (2) Poulet, G.; Pirre, M.; Maguin, F.; Ramaroson, R.; Le Bras, G. *Geophys. Res. Lett.* **1992**, *19*, 2305.
- (3) McElroy, M. B.; Salawitch, R. J.; Wofsy, S. C.; Logan, J. A. *Nature* **1986**, *321*, 759.
- (4) Garcia, R. R.; Solomon, S. *J. Geophys. Res.* **1994**, *99*, 12,937.
- (5) Wennberg, P. O.; Cohen, R. C.; Stimpfle, R. M.; Koplow, J. P.; Anderson, J. G.; Salawitch, R. J.; Fahey, D. W.; Woodbridge, E. L.; Keim, E. R.; Gao, R. S.; Webster, C. R.; May, R. D.; Toohey, D. W.; Avallone, L. M.; Proffitt, M. H.; Loewenstein, M.; Podolske, J. R.; Chan, K. R.; Wofsy, S. C. *Science* **1994**, *266*, 298.
- (6) Sander, S. P.; Ray, G. W.; Watson, R. T. *J. Phys. Chem.* **1981**, *85*, 199.
- (7) Danis, F.; Caralp, F.; Masanet, J.; Lesclaux, R. *Chem. Phys. Lett.* **1990**, *167*, 450.
- (8) Thorn, R. P.; Daykin, E. P.; Wine, P. H. *Int. J. Chem. Kinet.* **1993**, *25*, 521.
- (9) DeMore, W. B.; Sander, S. P.; Golden, D. M.; Hampson, R. F.; Kurylo, M. J.; Howard, C. J.; Ravishankara, A. R.; Kolb, C. E.; Molina, M. J. Chemical Kinetics and Photochemical Data for Use in Stratospheric Modeling; Evaluation Number 11, NASA JPL Publ. **1994**, No. 94–26.
- (10) Spencer, J. E.; Rowland, F. S. *J. Phys. Chem.* **1978**, *82*, 7.
- (11) Burkholder, J. B.; Ravishankara, A. R.; Solomon, S. *J. Geophys. Res.* **1995**, *100*, 16,793.
- (12) Hanson, D. R.; Ravishankara, A. R. *Geophys. Res. Lett.* **1995**, *22*, 385.
- (13) Patrick, R.; Golden, D. M. *Int. J. Chem. Kinet.* **1983**, *15*, 1189.
- (14) Anderson, L. C.; Fahey, D. W. *J. Phys. Chem.* **1990**, *94*, 644.
- (15) Rayez, M. T.; Destriau, M. *Chem. Phys. Lett.* **1993**, *206*, 278.
- (16) Shetter, R. E.; Davidson, J. A.; Cantrell, C. A.; Calvert, J. G. *Rev. Sci. Instrum.* **1987**, *58*, 1427.
- (17) Tyndall, G. S.; Orlando, J. J.; Calvert, J. G. *Environ. Sci. Technol.* **1995**, *28*, 202.
- (18) Cantrell, C. A.; Davidson, J. A.; McDaniel, A. H.; Shetter, R. E.; Calvert, J. G. *Chem. Phys. Lett.* **1988**, *148*, 358.
- (19) Tsalkani, N.; Toupance, G. *Atmos. Environ.* **1989**, *23*, 1849.
- (20) Atkinson, R.; Baulch, D. L.; Cox, R. A.; Hampson, R. F., Jr.; Kerr, J. A.; Troe, J. *J. Phys. Chem. Ref. Data* **1992**, *21*, 1125.
- (21) Schmeisser, M.; Fink, W.; Brändle, K. *Angew. Chem.* **1957**, *69*, 2085.
- (22) Schmeisser, M. *Inorg. Synth.* **1967**, *9*, 127.
- (23) Braun, W.; Herron, J. T.; Kahaner, D. K. *Int. J. Chem. Kinet.* **1988**, *20*, 51.
- (24) Islam, T. S. A.; Marshall, R. M.; Benson, S. W. *Int. J. Chem. Kinet.* **1984**, *16*, 1161.
- (25) Niki, H.; Maker, P. D.; Savage, C. M.; Breitenbach, L. P. *Int. J. Chem. Kinet.* **1985**, *17*, 525.
- (26) Nicovich, J. M.; Shackelford, C. J.; Wine, P. H. *J. Photochem. Photobiol., A: Chem.* **1990**, *51*, 141.
- (27) Soller, R.; Nicovich, J. M.; Wine, P. H. *XXII Informal Conference on Photochemistry*, Minneapolis, MN, June 1996.
- (28) Knauth, H.-D. *Ber. Bunsen-Ges. Phys. Chem.* **1978**, *82*, 212.
- (29) Knauth, H.-D. *Ber. Bunsen-Ges. Phys. Chem.* **1978**, *82*, 428.
- (30) Schonle, G.; Knauth, H. D.; Schindler, R. N. *J. Phys. Chem.* **1979**, *83*, 3297.
- (31) Chase, Jr., M. W.; Davies, C. A.; Downey, Jr., J. R.; Frurip, D. J.; McDonald, R. A.; Syverud, A. N. *J. Phys. Chem. Ref. Data* **1985**, *14*, 1.
- (32) Orlando, J. J.; Burkholder, J. B.; Bopagedara, A. M. R. P.; Howard, C. J. *J. Mol. Spectrosc.* **1991**, *145*, 278.
- (33) Durie, R. A.; Ramsay, D. A. *Can. J. Phys.* **1958**, *36*, 35.
- (34) Hanson, D. R.; Ravishankara, A. R.; Lovejoy, E. R., *J. Geophys. Res.* **1996**, *101*, 9063.
- (35) Orlando, J. J.; Burkholder, J. B. *J. Phys. Chem.* **1995**, *99*, 1143.
- (36) Monks, P. S.; Stief, L. J.; Krauss, M.; Kuo, S. C.; Klemm, R. B. *J. Chem. Phys.* **1993**, *100*, 1902.
- (37) McGrath, M. P.; Rowland, F. S. *J. Phys. Chem.* **1994**, *98*, 4773.
- (38) Ruscic, B.; Berkowitz, J. *J. Chem. Phys.* **1994**, *101*, 7795.
- (39) Lock, M.; Barnes, R. J.; Sinha, A. *J. Phys. Chem.* **1996**, *100*, 7972.

- (40) Thorn, R. P., Jr.; Stief, L. J.; Monks, P. S.; Kuo, S.-C.; Zhang, Z.; Klemm, R. B. Supplement to *EOS, Trans.* **1996**, 77, S47.
- (41) Glukhovtsev, M. N.; Pross, A.; Radom, L. *J. Phys. Chem.* **1996**, 100, 3498.
- (42) Kukui, A.; Kirchner, U.; Benter, Th.; Schindler, R. N. *Ber. Bunsen-Ges. Phys. Chem.* **1996**, 100, 455.
- (43) Lee, T. J. *J. Phys. Chem.* **1995**, 99, 15074.
- (44) Lee, T. J. *J. Phys. Chem.* **1995**, 99, 1943.
- (45) Chambers, R. M.; Heard, A. C.; Wayne, R. P. *J. Phys. Chem.* **1992**, 96, 3321.
- (46) Radlein, D. St. A. G.; Whitehead, J. C.; Grice, R. *Nature* **1975**, 253, 37.
- (47) Reddy, R. R.; Rao, T. V. R.; Reddy, A. S. R. *Indian J. Pure Appl. Phys.* **1989**, 27, 243.
- (48) McGrath, M. P.; Rowland, F. S. *J. Phys. Chem.* **1996**, 100, 4815.
- (49) Gilles, M. K.; Turnipseed, A. A.; Talukdar, R. K.; Rudich, Y.; Villalta, P. W.; Huey, L. G.; Burkholder, J. B.; Ravishankara, A. R. *J. Phys. Chem.* **1996**, 100, 14005.
- (50) Bedjanian, Y.; Le Bras, G.; Poulet, G. *J. Phys. Chem.* **1996**, 100, 15130.
- (51) Zhang, Z.; Monks, P. S.; Stief, L. J.; Liebman, J. F.; Huie, R. E.; Kuo, S.-C.; Klemm, R. B. *J. Phys. Chem.* **1996**, 100, 63.
- (52) Troe, J. *J. Chem. Phys.* **1977**, 66, 4758.
- (53) Troe, J. *J. Phys. Chem.* **1979**, 83, 114.
- (54) Troe, J. *J. Chem. Phys.* **1981**, 75, 226.

JP9620274